RAPID COMMUNICATIONS

PHYSICAL REVIEW B VOLUME 44, NUMBER 8 15 AUGUST 1991-II

# Effect of valence-subband structure on the energy relaxation dynamics of electrons in GaAs quantum wells grown on Si

Kai Shum, Y. Takiguchi, J. M. Mohaidat, and R. R. Alfano
*Institute for Ultrafast Spectroscopy and Lasers, Electrical Engineering Department and Physics Department, The City College of New York, New York 10031*

K. Adomi and H. Morkoc
*Coordinated Science Laboratory, University of Illinois at Urbana-Champaign, 1101 West Springfield Avenue, Urbana, Illinois 61801*

(Received 9 October 1990; revised manuscript received 3 June 1991)

Different electron energy relaxation dynamics are observed in narrow and wide modulation Be-doped GaAs-$Al_xGa_{1-x}As$ multiple quantum wells grown on Si substrates (GaAsQW's/Si) arising from different valence subband structure. The combination of built-in biaxial stress and spatial hole confinement results in a reversal of light- and heavy-hole subbands in narrow GaAsQW's/Si structures. For narrow (wide) quantum-well structures of 40 (188) Å at 4.3 K in which there is a two-dimensional light- (heavy-) hole gas, the energy-loss process of photoexcited hot electrons is extremely rapid (slow) due to strong (weak) energy exchange with the cool light (heavy) holes. The nonequilibrium phonon population was found to build up from the relaxation of hot electrons in the 188-Å wells but not in the 40-Å wells.

Recently, the dynamics of photoexcited hot carriers has been extensively studied[1-5] in GaAs quantum wells (QW's) *grown on a lattice-matched GaAs substrate* because of their technological importance in the development of optoelectronic devices. The carrier dynamics has not been extensively investigated so far in GaAs QW's *grown on a lattice-mismatched Si substrate.* There are two reasons why it is important to study the electron dynamics in GaAsQW's/Si. First, GaAsQW's/Si is a prototype structure of possible monolithic integration of *(III-V)*-semiconductor-based transistors, lasers, and optoelectronic devices on a single chip. Second, the existence of biaxial stress at given lattice temperature arising from the difference between thermal expansion coefficients of GaAs epilayers and Si substrate causes the valence subband configuration to be substantially changed by varying the width of the QW's. In a narrow GaAsQW/Si, the light-hole (lh) subband can be above the heavy-hole (hh) subband while in a wide GaAsQW/Si the reverse is true. In a GaAs QW/GaAs, however, whether doped or not, the population of the hh's is always larger than that of the lh's. The unique valence subband tunability in GaAsQW's/Si by the stress and spatial hole confinement can change the relative population of lh's and hh's with which the photoexcited hot electrons can interact. When the lh's (hh's) reside in the wells, photoexcited hot electrons strongly (weakly) exchange energy with lh's (hh's) along with longitudinal optical (LO) phonon emission process. If the energy exchange rate for the electron-hole interaction is much greater (smaller) than that for electron–LO-phonon interaction, a nonequilibrium LO-phonon population could not (could) be built up resulting in a rapid (slow) electron energy relaxation. Therefore, it is expected that from the effects of valence subband structure one can gain a deeper understanding of the electron dynamics in GaAs QW's and control the transport of carriers.

In this paper, the experimental results of time-resolved photoluminescence spectroscopic measurements are reported on *the electron energy relaxation dynamics* in two QW structures with different valence subband configurations: a 188-Å multiple QW structure with doped-in hh's and a 40-Å multiple QW structure with doped-in lh's. It was found that for the 40 (188) Å wells in which a two-dimensional (2D) lh (hh) gas resides, the energy-loss process of photoexcited electrons is rapid (slow) due to strong (weak) energy exchange between the hot electrons and the cool lh's (hh's).

The QW structures were grown by molecular-beam epitaxy on a (100) silicon substrate 4° tilt toward [011] with a 2-$\mu$m GaAs buffer layer. The same barriers ($Al_xGa_{1-x}As$) are used for the two QW structures. Both QW structures are repeated for 20 periods. The composition $x$ is 0.35. The barrier thickness is 250 Å in which a central region of 50 Å is doped with Be atoms. The doping in the barriers provides a lh density of $1.9\times10^{12}$ $cm^{-2}$ in the 40-Å wells with a Fermi energy ($E_{Fh}$) of 40.3 meV and a similar density of $2.5\times10^{12}$ $cm^{-2}$ for hh's in the 188-Å wells with $E_{Fh}=12$ meV. It should be noted that the numbers for the composition, layer thickness, and doping densities are the nominal values.

In order to make clear how the different hole subband configuration for the two QW structures occurs, the valence-band structure of the 2-$\mu$m GaAs/Si QW is first inspected. Due to the biaxial stress caused by the difference between the thermal expansion coefficients of the GaAs epilayer and the Si substrate, the $J=\frac{3}{2}$ valence band of the 2-$\mu$m GaAs is decoupled into $m_j=\pm\frac{1}{2}$ and $m_j=\pm\frac{3}{2}$ bands.[6,7] The $k$-dependent parts of the valence-band energies are given to the lowest order in $\mathbf{k}$:

$$E_{\pm1/2}=\frac{\hbar^2}{2m_0}[(\gamma_1-\gamma_2)(k_x^2+k_y^2)+(\gamma_1+2\gamma_2)k_z^2], \quad (1a)$$

$$E_{\pm3/2}=\frac{\hbar^2}{2m_0}[(\gamma_1+\gamma_2)(k_x^2+k_y^2)+(\gamma_1-2\gamma_2)k_z^2], \quad (1b)$$

where $\gamma_1$, $\gamma_2$ (6.85, 2.1) are Luttinger parameters for GaAs. Schematic representation of Eq. (1) is shown in Fig. 1(a). The hole mass of the $\pm\frac{1}{2}$ band is heavier in the $x$-$y$ plane than in the $z$ direction (growth direction [100]) while the reverse is true for the $\pm\frac{3}{2}$ band. The biaxial-stress-induced energy separation $\Delta E_H$ between the $\pm\frac{1}{2}$ and $\pm\frac{3}{2}$ bands is about 14 meV at 4 K. Because of the QW potential the $m_j=\pm\frac{1}{2}$ and $m_j=\pm\frac{3}{2}$ states are quantized along the [100] QW growth direction. The quantization energies strongly depend on the well width and hole masses in both well and barrier. Based on Fig. 1(a), two extreme cases can be identified for the valence subband configuration of QW structures: (i) when the well is very thick so that the energy difference $\Delta E_{QW}$ between the quantization energies of $\pm\frac{1}{2}$ and $\pm\frac{3}{2}$ states are very small; and (ii) when the well is about 40 Å thick so that the $\Delta E_{QW}$ reaches a maximum.[8] For the GaAs QW's on 2-$\mu$m GaAs on Si substrate, the energy separation between $\pm\frac{1}{2}$ and $\pm\frac{3}{2}$ subbands is given by

$$\Delta E=\Delta E_H-\Delta E_{QW}. \quad (2)$$

In the case of the 40-Å QW's as shown in Fig. 1(b), $\Delta E$ is negative when $\Delta E_{QW}$ exceeds $\Delta E_H$ resulting in a reverse of the lh and the hh subbands in QW plane. While for the 188-Å wells [Fig. 1(c)], $\Delta E$ is positive when $\Delta E_{QW}$ is less than $\Delta E_H$ reflecting a normal order of hole subbands, i.e., the lh subband is below the hh subband. It should be emphasized that Fig. 1 is meant to be schematic. Neither any admixture of $\pm\frac{1}{2}$ and $\pm\frac{3}{2}$ states nor anticrossing effects are considered. The Fermi levels indicated in Figs. 1(b) and 1(c) are first estimated based on the doping densities and then verified by spectrum fitting.

The QW structures at 4.3 K were photoexcited by a train of 80-fs 620-nm laser pulses from a colliding-pulse mode-locked laser operated at 82 MHz with an average power of 5 mW. The photoluminescence (PL) at an excitation density of $\sim 10^{16}$ cm$^{-3}$ was dispersed by a 0.22-m monochromator and detected by a 2D Hamamatsu $S$-1 synchroscan streak camera with a system time resolution of 7 ps and a spectral resolution of 1 nm.

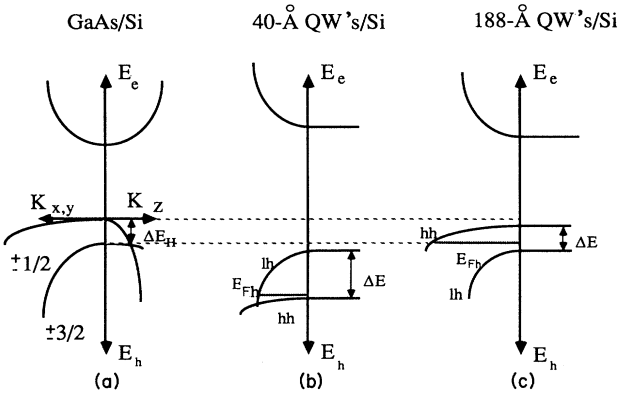


FIG. 1. Schematic energy-band diagrams for the 2-$\mu$m GaAs, 40-Å GaAs multiple quantum well (MQW), and 188-Å GaAs MQW grown on Si substrate. Note that the anticrossing effect is not considered here.

The time- and wavelength-resolved PL spectra for the 40- and the 188-Å wells are displayed in Figs. 2(a) and 2(b), respectively. The slow turn-on of the luminescence peak intensity for the 40-Å wells may be due to the migration of photoexcited electrons to larger islands; while for 188-Å wells it is due to the slow electron energy relaxation which will be discussed later. The 40-Å well spectra clearly show two distinct peaks arising from $n=1$ electron to lh (low-energy side) and hh (high-energy side) transitions with an energy separation of 41 meV. The 188-Å well spectra also show the $n=1$ electron to hh transition with a small shoulder on the high-energy side of the PL originating from the $n=1$ electron to lh transition. The measured spectra for both 40- and 188-Å QW structures are consistent with the hole subband configurations indicated in Figs. 1(b) and 1(c). In the case of the 40-Å wells, the measured value of $-41$ meV for $\Delta E$ implies a value of 55 meV for $\Delta E_{QW}$. This value is larger than what would be predicted based on the nominal structure parameters and the masses inferred from Eq. (1). Since the value of $\Delta E_{QW}$ in a sensitive well width range[8] depends critically on many parameters such as band offset and ratio of hh to lh mass, a precise prediction is difficult. However, it is certain that the $\pm\frac{1}{2}$ and $\pm\frac{3}{2}$ bands in $x$-$y$ plane for 40-Å QW's/Si are reversed in comparison with GaAs/Si. Lighter hole mass for the $\pm\frac{3}{2}$ subband in $x$-$y$ plane is also consistent with larger Fermi energy in this structure. The electron to hh and lh transitions in the 188-Å QW's/Si are not resolved. This is also consistent with Eq. (1), which predicts a small positive value for $\Delta E$ because $\Delta E_{QW}$ is small for the thick QW's.

In order to obtain quantitative information about the effects of valence-band structures on the electron energy relaxation processes, the electron temperatures at different times (cooling curve) are determined from a careful analysis of time-resolved PL spectra. Our theoretical model for calculating PL spectra [$I_{PL}(E, T_e, T_{hh}, T_{lh})$]

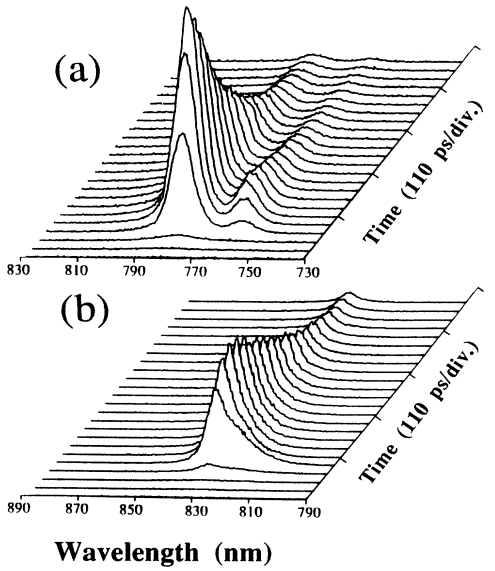


FIG. 2. Time-resolved PL spectra at 4.3 K for (a) 40-Å MQW's/Si, and (b) 188-Å MQW's/Si.

consists of the following assumptions: excitonic many-body effects can be neglected because of large doped-in hole density in both structures;[9,10] spontaneous transition rate[11] $W(E, T_e, T_{hh}, T_{lh})$ is calculated by Fermi's "golden rule"; carriers (electron, hh, lh) obey Fermi-Dirac distributions with different temperatures ($T_e$, $T_{hh}$, $T_{lh}$); and a probability density function $G(E)$ is used which is transferred from a Gaussian function for the well width fluctuation[12] and the other energy-level broadenings are described by a Lorentzian factor $L(E)$. The theoretical PL spectra with different values of $T_e$, $T_{hh}$, and $T_{lh}$ are obtained by convoluting $W(E, T_e, T_{hh}, T_{lh})$ with $G(E)$ and $L(E)$:

$$I_{PL}(E, T_e, T_{hh}, T_{lh}) = W(E, T_e, T_{hh}, T_{lh}) * G(E) * L(E) . \quad (3)$$

Comparing the calculated $I_{PL}(E, T_e, T_{hh}, T_{lh})$ and measured $I_{PL}(E, t)$, the electron, hh, and lh temperatures at different times are experimentally determined.

Two typical comparisons between the measured and calculated spectra for the 188-Å wells and the 40-Å wells are shown in Figs. 3(a) and 3(b), respectively. The calculated PL can fit the measured spectrum of the 188-Å wells at 37 ps using values of 67, 67, and 4.3 K for the electron, lh, and hh temperatures, respectively. The spectral region below the onset of the $n=1$ electron to lh transition is very sensitive to the choice of electron temperatures, while lh temperature is dictated by the high-energy tail of $n=1$ electron to lh recombination. It should be pointed out that the first and second lh subbands must be used in order to obtain the excellent fit. To fit the measured spectrum of the 40-Å wells at 29 ps, $T_e=15.3$ K, $T_{hh}=T_{lh}=T_h=7.3$ K are required for the electron and hole temperatures, respectively. Since the photogenerated hot hh's can quickly lose their excess energy to the cool doped-in lh's in the 40-Å wells, both types of holes have reached into the equilibrium state within our time resolution in contrast to the holes in the 188-Å wells. The intensity of the $n=1$ electron to hh emission peak in the 40-Å wells is extremely sensitive to the hole temperature $T_h$ because the quasi-Fermi level for the hole system is 0.6 meV below the hh subband edge where the density of states for the hh's is large. From the overall comparison of the calculated and measured spectra, three conclusions are reached: the electron temperature in the 188-Å wells is much hotter than in the 40-Å wells; the hh's and lh's in the 40-Å wells can be described by a common hole temperature $T_h$ which is slightly elevated above 4.3 K; and the temperature for the electrons and the lh's is different and higher than the hh temperature which remains 4.3 K in the 188-Å wells.

The electron temperature cooling data obtained from the line fitting are plotted in Fig. 4 as circles for the 188-Å wells and squares for the 40-Å wells. The data-point size along the time axis reflects the finite time resolution. The estimated error on the electron temperature for the 188-Å wells is indicated by vertical bar (when it is larger than data-point size). The main source for the error arises from the lack of precise values for the hh and lh masses which determine the partition of excess energies for electrons and holes as well as the radiative transition rates. The size of error for the 188-Å wells at the earlier time is relatively large because the high-energy side of spectra covers many hole subbands, while for the 40-Å wells the error is small since only two hole subbands are involved in line fitting.

Inspection of Fig. 4 reveals that the maximum obtainable electron temperature (~30 K) in the 40-Å wells is below 40 K with the present time resolution. This low initial electron temperature indicates that the hot-electron energy relaxation process by emission of LO phonons is over within our time resolution. We attribute this rapid initial electron energy relaxation process to the strong energy exchange between the *hot electrons* and the doped-in *cool lh's*. Since most of the excess energy of photogenerated electrons is shared with the cool lh's nonequilibrium phonon population may not have any chance to be built up. The cooling from 30 to 4.3 K within ~100 ps strongly supports the electron-to-lh energy-loss mechanism. For the electron temperature below 30 K, the electron energy loss by the emission of LO phonon is negligi-

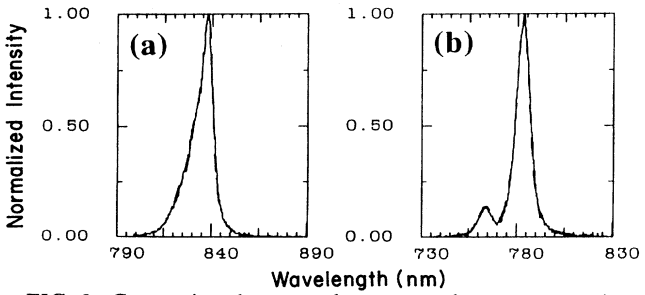


FIG. 3. Comparison between the measured spectrum at given time (solid curves) and theoretically calculated spectrum with given electron, hh, and lh temperatures (dot-dashed curves). (a) For 188-Å QW's at 37 ps; $T_e=67$ K, $T_{lh}=67$ K, and $T_{hh}=4.3$ K. (b) For 40-Å QW's at 29 ps; $T_e=15.3$ K and $T_h=7.3$ K.

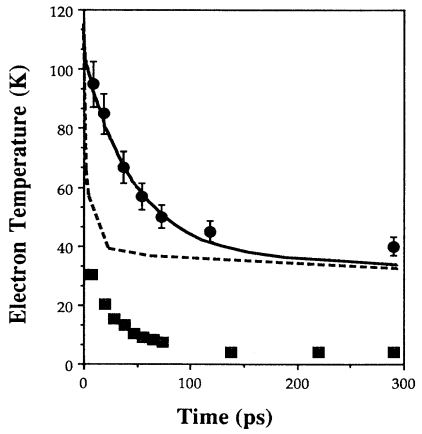


FIG. 4. Electron cooling curves for the 188-Å QW's (circles) and 40-Å QW's (squares). The solid and dashed curves are the theoretical calculations with and without the nonequilibrium-phonon effects, respectively. The time scale of this figure is chosen not to correlate with that of Fig. 2 because there is no further cooling about 100 ps after the photoexcitation in the time scale we work with. The zero time was determined by the scattered excitation light from the sample surface.

ble. It should also take several tens of nanoseconds to cool the electron temperature from 30 to 4.3 K if acoustic phonons are responsible for the electron energy loss. As a striking contrast, the maximum obtainable electron temperature in the 188-Å wells in which the hh's are doped-in instead of the lh's is about 95 K, an electron temperature at which the LO-phonon emission process is a dominant energy-loss mechanism for the hot electrons. The electron temperature cooling is slower than expected on the basis of equilibrium LO phonon and electron interaction. The slow hot-electron energy relaxation in the 188-Å wells is due to the weak energy exchange between the hot electrons and the cool hh's so that the hot electrons can lose their excess energy mainly by the LO-phonon emission channel. Although the initial cooling (0–1 ps) of hot electrons is rapid by emitting LO phonons, those emitted LO phonons will soon accumulate due to their finite lifetime and become the hot LO-phonon reservoir with which the hot electrons are attempting to reach equilibrium. This feedback results in slower hot-electron cooling on a time scale of 100 ps in the 188-Å QW's.

In order to further confirm that: (i) the nonequilibrium phonon population is built up in the 188-Å QW's, and (ii) the electron-lh interaction is a dominant electron energy-loss mechanism in the 40-Å QW's, a simple theoretical analysis[13] is given to compare with the experimental hot-electron cooling curves in Fig. 4. The electron and nonequilibrium LO-phonon temperatures are calculated by two coupled differential equations:

$$\partial T_e/\partial t = -P_0 F(T_e,T_p)\,, \tag{4}$$

$$\frac{\partial T_p}{\partial t} = P_0 F(T_e,T_p) - \frac{N(T_p)}{\tau_p}\frac{\partial T_p}{\partial N(T_p)}\,. \tag{5}$$

The function $F(T_e,T_p)$ is given by[14]

$$F(T_e,T_p) = \frac{e^{x_p - x_e}-1}{e^{x_p}-1}(x_e/\pi)^{1/2} e^{x_e/2} K_0(x_e/2)\,, \tag{6}$$

where $x_{p,e} = E_{\rm LO}/k_B T_{p,e}$ and $K_0$ is the modified Bessel function of zero order. The material parameter: $P_0 = 3.54\times 10^{11}[E_{\rm LO}({\rm meV})]^{3/2}(m_e^*/m_0)^{1/2}[(1/\epsilon_\infty)-1/\epsilon_0]$ (eV/s) is calculated to be 3.16 K/ps for GaAs. $N(T_p)$ is the Bose-Einstein factor appropriate to LO phonons of energy $E_{\rm LO}$. The LO-phonon lifetime is denoted by $\tau_p$.

The numerical solution of the coupled differential equations [Eqs. (4) and (5)] yields the temporal dependence of the electron temperature shown as the solid and dashed curves in Fig. 4 for the *electron–nonequilibrium-phonon* and the *electron–equilibrium-phonon* interactions, respectively. The initial electron temperature of 200 K is used for both theoretical curves while the phonon lifetime $\tau_p$ is 8 ps for the solid curve and 0 ps for the dashed curve. It should be pointed out that the above analysis does not take the effects of well thickness (confinement) and holes into account. Good fit between the theoretically calculated solid curve with the experimental data for 188-Å QW's demonstrates that the nonequilibrium-phonon population is indeed responsible for the slow hot-electron relaxation in 188-Å QW's. The calculated dashed curve clearly indicates the following: (i) the high initial electron temperature will rapidly decrease below 40 K in a few picoseconds when the nonequilibrium LO-phonon population is absent; (ii) after a few picoseconds the photoexcited hot electrons will remain hot at above 30 K for several 100 ps when the electron-lh interaction is switched off. Our interpretation of the experimental data for 40-Å QW's is consistent with the above analysis.

In conclusion, we have presented an experimental investigation of the effect of valence subband structure on the hot-electron energy relaxation process in GaAs QW's grown on Si substrate. It was demonstrated that for the 40 (188) Å QW structure in which 2D 4.3-K lh (hh) gas exists, the energy-loss process of photoexcited electrons is rapid (slow) due to strong (weak) energy exchange between the hot electrons and cool lh's (hh's). The nonequilibrium-phonon population was built up in the process of hot-electron relaxation for the 188-Å wells but not for the 40-Å wells. Under some photoexcitation conditions, it seems that we can control the hot-electron energy relaxation process in GaAs QW's/Si by interchanging the hh and lh subbands. This provides a critical experimental test of the existing theories on hot carrier energy relaxation processes. Further work is needed to time resolve the initial electron energy relaxation in a femtosecond time scale and to carry out the theoretical calculation of hot-electron cooling due to the electron-lh interaction with Fermi statistics at low temperatures.

We gratefully acknowledge the support of NSF Grant No. ECS-8819651 and Hamamatsu Photonics.

[1] C. V. Shank *et al.*, Solid State Commun. **47**, 981 (1982).
[2] Jagdeep Shah *et al.*, Phys. Rev. Lett. **54**, 2045 (1985).
[3] J. F. Ryan *et al.*, Phys. Rev. Lett. **53**, 1841 (1984).
[4] Kai Shum *et al.*, Phys. Rev. B **37**, 8923 (1988).
[5] K. Leo, W. W. Ruhle, and K. Ploog, Phys. Rev. B **38**, 1947 (1988).
[6] S. Zemon *et al.*, Solid State Commun. **58**, 457 (1986).
[7] A. Freunidlich *et al.*, Phys. Rev. B **40**, 1652 (1989).
[8] K. Shum, P. P. Ho, and R. R. Alfano, Phys. Rev. B **33**, 7259 (1986).
[9] S. Schmitt-Rink, C. Ell, and H. Haug, Phys. Rev. B **33**, 1183 (1986).
[10] T. Uenoyama and L. J. Sham, Phys. Rev. Lett. **65**, 1048 (1990). According to their calculation, excitonic many-body effect is not important when the effective-mass ratio between electron and hole is close to 1. This is the case for the 40-Å wells.
[11] H. C. Casey, Jr. and M. B. Panish, *Heterostructure Lasers (Part A)* (Academic, New York, 1978).
[12] K. Shum, P. P. Ho, R. R. Alfano, D. F. Welch, G. W. Wicks, and L. F. Eastman, IEEE J. Quantum Electron. **QE-22**, 1811 (1986).
[13] H. M. van Driel, Phys. Rev. B **19**, 5928 (1979).
[14] J. Shah and R. F. Leheny, in *Semiconductor Probed by Ultrafast Laser Spectroscopy,* edited by R. R. Alfano (Academic, New York, 1984).